

Beta decay of  $^{99}\text{Tc}^m$ 

D. E. Alburger, P. Richards, and T. H. Ku

Brookhaven National Laboratory, Upton, New York 11973

(Received 9 October 1979)

The emission of  $\beta$  rays from 6.02-h  $^{99}\text{Tc}^m$  has been detected with an intermediate-image magnetic spectrometer.  $\beta$ -ray components with end-point energies of  $434.8 \pm 2.6$  keV ( $\beta_0$ ) to the  $^{99}\text{Ru}$  ground state and  $346.7 \pm 2.0$  keV ( $\beta_1$ ) to the 90-keV state were found with intensities per decay of  $(1.0 \pm 0.3) \times 10^{-5}$  for  $\beta_0$  and  $(2.6 \pm 0.5) \times 10^{-5}$  for  $\beta_1$ . In the Kurie plot analysis the unique first-forbidden "a" shape was assumed for  $\beta_0$  and an allowed shape was assumed for  $\beta_1$ . Values of  $\log f_0 t = 9.39 \pm 0.11$  for  $\beta_0$  and  $\log f_1 t = 8.66 \pm 0.08$  for  $\beta_1$  were derived.  $\gamma$  rays of 322, 233, and 140 keV were observed in a calibrated Ge(Li) detector with relative source intensities of  $I_{322}:I_{233}:I_{140} = (1.13 \pm 0.09) \times 10^{-6}:(0.95 \pm 0.17) \times 10^{-7}:1.000$ . The total  $\beta$ -ray branching of  $3.7 \times 10^{-5}$  results in a negligible correction to dosage calculations in the use of  $^{99}\text{Tc}^m$  for diagnostic nuclear medicine.

[RADIOACTIVITY  $^{99}\text{Tc}^m$ : measured  $E_\beta$ ,  $I_\beta$ , and  $I_\gamma$ ; magnetic spectrometer, Ge(Li); deduced decay scheme.]

## I. INTRODUCTION

$^{99}\text{Tc}^m$  is an activity of 6.02-h half-life known<sup>1</sup> to decay by isomeric transitions of either 2.1 keV ( $E3$ , 98.6%) or 142.6 keV ( $M4$ , 1.4%). The 2.1-keV transition is followed by one of 140.5 keV which emits either 140.5-keV  $\gamma$  rays (89.4%) or internal conversion electrons (10.6%) leading to the ground state of  $^{99}\text{Tc}$ . There is extensive usage of  $^{99}\text{Tc}^m$  as a radiopharmaceutical in diagnostic nuclear medicine<sup>2</sup> and it is important in such applications to fully understand the decay scheme. Although an energy of 436 keV is available for the  $\beta$  decay of  $^{99}\text{Tc}^m$  to  $^{99}\text{Ru}$ , there have been no reported direct measurements of  $\beta$ -ray emission. However, from the presence of low-intensity  $\gamma$  rays of 322 keV, a  $\beta$ -ray branch<sup>3,4</sup> of  $(1.0 \pm 0.1) \times 10^{-6}$  per decay to the 322-keV state of  $^{99}\text{Ru}$  has been inferred.<sup>5</sup> This would be a unique first-forbidden transition of  $\beta_{\max} = 113.8$  keV from  $^{99}\text{Tc}^m$ , which has a spin-parity  $J^\pi = \frac{1}{2}^-$  to the  $^{99}\text{Ru}$  322-keV state which probably has  $J^\pi = \frac{5}{2}^+$ . Since the  $^{99}\text{Ru}$  ground state is of  $J^\pi = \frac{5}{2}^+$  and the 90-keV first-excited state is  $\frac{3}{2}^+$ , the corresponding  $\beta$  transitions are unique first-forbidden for  $\beta_0$  and nonunique first forbidden for  $\beta_1$ . But due to their higher end-point energies, i.e., 436.2 keV for  $\beta_0$  and 346.4 keV for  $\beta_1$ , based on the known mass excesses and level schemes,<sup>1</sup> the intensities of these branches are expected to be considerably greater than the  $\beta$  branch to the 322-keV state. The present measurements were carried out in order to search for these  $\beta$ -ray branches so as to obtain more complete information on the decay scheme of  $^{99}\text{Tc}^m$  and to see if significant corrections might be needed in dosage calculations for

nuclear medicine applications.

As noted in the Discussion, there is conflicting evidence between the  $\beta$ -ray branching intensity of  $^{99}\text{Tc}^m$  to the 322-keV state of  $^{99}\text{Ru}$  and the spin assignment to that state. Although two<sup>3,4</sup> of the previous measurements of that  $\beta$ -ray branch have been in agreement, it was felt that a further check would be desirable, as well as a search for the 233-keV cascade  $\gamma$  ray (322  $\rightarrow$  90) from the 322-keV state.  $\gamma$ -ray measurements on  $^{99}\text{Tc}^m$  have therefore been carried out. An abbreviated report of the present results has been given elsewhere.<sup>6</sup>

## II. EXPERIMENTAL PROCEDURES

The instrument used for measuring the  $\beta$ -ray spectrum of  $^{99}\text{Tc}^m$  was an iron-free intermediate-image magnetic spectrometer.<sup>7</sup> As in recent measurements on the  $\beta$ -ray spectra of  $^{20}\text{F}$  (Ref. 8) and  $^{28}\text{Mg}$  (Ref. 9), the detecting system at the final focal point of the spectrometer consisted of an anthracene crystal 2 mm thick and 20 mm in diameter on the end of a light pipe.  $\beta$  rays focused onto the detector produce a pulse-height spectrum from an RCA-6342 photomultiplier tube, at the other end of the light pipe, characterized by a peak plus a low-energy tail. For a given set of measurements a fixed low-energy bias is applied to the pulse-height spectrum to exclude noise and low-energy background counts.

Spectrometer sources of  $^{99}\text{Tc}^m$  were prepared by evaporating a saline solution containing the activity to dryness on an aluminum support foil 2.4 mg/cm<sup>2</sup> in thickness. The spot of active material was  $\sim 7$  mm in diameter and estimated to be a few mg/cm<sup>2</sup> in thickness. It was mounted

in the normal source position in the spectrometer.

Standard procedures were used to record the  $\beta$ -ray spectrum, i.e., for a given magnetic field setting the number of counts and counting interval were recorded as well as the clock time for later decay corrections. Spectrum points were interleaved in order to check for any systematic variations and data points were taken beyond the spectrum endpoint for background subtraction. At all data points the detector spectrum was monitored with a pulse-height analyzer.

Several supplementary measurements were made on the spectrometer for later use in the calculations. All of these tests made use of a thin electroplated source of  $^{207}\text{Bi}$  6 mm in diameter. The momentum calibration, in G cm per unit of coil current, and the instrumental line width were determined from the K-570 internal conversion line. At the maximum spectrometer transmission setting, as used in this work, the full width at half maximum of the conversion line was 4.4% in momentum. This width was needed in analyzing the fraction of the total spectrum that is detected within the instrumental line width at a given point on the  $^{99}\text{Tc}^m$   $\beta$ -ray spectrum.

Another factor that enters the calculations is the absolute spectrometer transmission. Previous measurements<sup>7</sup> at the maximum transmission setting, using a point source of  $^{207}\text{Bi}$  and a Geiger counter detector 2.9 cm in diameter, gave a value of 8.0% of  $4\pi$  for the transmission. However, with an extended source of 6 mm diameter and a detector of 2.0 cm diameter it was thought that the final image could be a bit larger in diameter than the detector so that the effective transmission might be reduced somewhat. Under these conditions inexact alignment of the detector could further reduce the effective transmission. Also, two support legs for additional lead shielding have been added inside the spectrometer since the original measurements were made and these will reduce the transmission slightly. The present determination of transmission consisted of finding the peak counting rates when focusing either the K-570 or K-1064 keV internal conversion lines from the 6-mm diameter  $^{207}\text{Bi}$  source and correcting for the number of counts below the bias by recording the pulse-height spectrum with and without the bias imposed. The rates of 570- and 1064-keV  $\gamma$ -ray emission from this same source were then measured with a  $12.7 \times 12.7$  cm NaI(Tl) detector at source-to-crystal distances of 10.0 and 20.0 cm by recording the net number of counts in the corresponding full-energy-loss peaks and correcting for  $\gamma$ -ray absorption in the Al container, for scaler dead time, and for the absolute photopeak efficiency<sup>10</sup> for this size crys-

tal at the corresponding  $\gamma$ -ray energy. Results for the intensities of the two  $\gamma$  rays at the two distances were consistent within their errors with each other and with the known decay scheme<sup>1</sup> of  $^{207}\text{Bi}$ . By using the known K-conversion coefficients,<sup>1</sup> i.e.,  $e_K/\gamma = 0.0159$  for the 570-keV transition and  $e_K/\gamma = 0.0985$  for the 1064-keV transition, the K-conversion emission rates were calculated. Combining these rates with the spectrometer measurements, the resulting transmissions for the 570- and 1064-keV transitions were in good agreement and a value of  $6.6 \pm 0.4\%$  of  $4\pi$  was determined for the effective spectrometer transmission under the conditions used for the  $^{99}\text{Tc}^m$  experiments.

The  $\gamma$ -ray spectrum of  $^{99}\text{Tc}^m$  was measured using a Ge(Li) detector of coaxial cylindrical shape having an efficiency of 15.3% relative to a  $7.62 \times 7.62$ -cm NaI(Tl) detector for 1.33-MeV  $\gamma$  rays. In order to determine the calibration of photopeak efficiency versus  $\gamma$ -ray energy, a source of  $^{169}\text{Yb}$  was used. This activity emits<sup>1</sup> a convenient set of six  $\gamma$  rays of known relative intensities covering the energy range 109.8 to 307.7 keV. Further details of these measurements are described below.

### III. RESULTS

#### A. $\beta$ -ray spectrum

Data points for the  $\beta$ -ray spectrum of  $^{99}\text{Tc}^m$  could be measured reliably in the  $\beta$ -ray spectrometer only above a focusing energy of about 200 keV. As the focusing energy was reduced, starting at about 220 keV, it was noted in the pulse-height spectrum of the anthracene detector that there was a low-energy rise in the tail below the peak of the spectrum. This rise was attributed to the production of secondary electrons in the spectrometer baffle system by the 140.5-keV  $\gamma$  rays and the scattering of these electrons into the detector. Corrections were made at each momentum setting by an analysis of the pulse-height spectrum and were included in the overall detector efficiency that depended on the bias setting. But as the focusing energy was reduced below 200 keV the scattering effect became so severe and the corrections so large that the data points could not be used. Contributing to the problem was the fact that the decrease in focusing energy also lowers the pulse-height of the main peak towards the region of increasing background yield. Hence the measurements were confined to  $\beta$ -ray energies extending from 210 to 630 keV. Between 450 and 630 keV five points were taken forming a flat background amounting to an average rate of about 2% of the net rate at 210 keV.

In the final experiments two successive runs were made on the  $^{99}\text{Tc}^m$   $\beta$ -ray spectrum, the first of 2 min per point and the second 3 min per point giving comparable statistics. In the second run the pulse-height bias on the detector output was set higher than in the first run so as to further discriminate against low-energy background (but this resulted in a somewhat lower overall efficiency). The data of the separate runs were analyzed by subtracting the corresponding flat background value from each point and correcting for decay using a half-life value of 6.02 h. A curve of detector efficiency versus focused  $\beta$ -ray energy was developed for each of the two biases by making an analysis of the various pulse-height spectra. In all cases the efficiency was  $>90\%$  but for each of the two biases the maximum variation in detector efficiency over the total region was about 5%. The efficiency curve for the higher bias used in the second run was about 4% lower than for the first run at lower bias. When the efficiency corrections were made, the final fully corrected data points for the separate runs were in excellent agreement, and their sums, normalized to 4 min per point, are shown by the points in Fig. 1(a). While the yield from the magnetic spectrometer is actually proportional to the  $\beta$  intensity per unit momentum interval times the momentum setting, the points in Fig. 1(a) are plotted versus electron energy (instead of momentum) so as to correspond to the Kurie plots of curve (b).

#### B. $^{99}\text{Tc}^m$ source strength for $\beta$ -ray measurements

Since the  $^{99}\text{Tc}^m$  source used for the final set of  $\beta$ -ray measurements was quite strong, the determination of its strength was made 27 h after the beginning of the  $\beta$ -ray experiments when it had decayed to about 4% of the initial value. Even then the source had to be located 200 cm from either a  $12.7 \times 12.7$ -cm or a  $7.62 \times 7.62$ -cm NaI(Tl) detector to keep the counting rate due to the 140.5-keV  $\gamma$  rays down to an acceptable level. The procedure was to measure the net counting rate of the 140.5-keV photopeak and to correct for the absolute photopeak efficiency,<sup>10</sup> for scaler deadtime, and for  $\gamma$ -ray absorption both in the Al container of the detector and in 2 m of air. These two absorption corrections amounted to a total of 6.2%. Results for the two NaI(Tl) detector sizes were in excellent agreement. The  $\gamma$ -ray emission rate was corrected for the fraction of  $\gamma$ 's per 140.5-keV transition (89.4%), for the 140.5-keV transition branching intensity of 98.6%, and for the amount of decay in order to derive the total disintegration rate at the beginning of the  $\beta$ -ray measurements. Owing to the high internal conversion<sup>1</sup> of the 142.6-keV  $M4$  crossover tran-

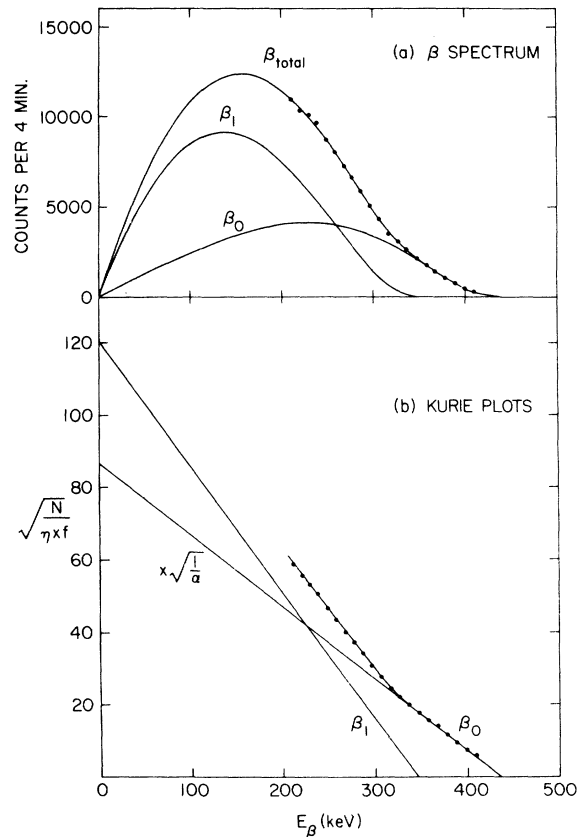


FIG. 1. (a)  $\beta$ -ray spectrum of  $^{99}\text{Tc}^m$  including experimental data points, constructed components, based on curve (b), and constructed total spectrum. (b) Kurie plot analysis assuming the unique first-forbidden " $\alpha$ " shape for  $\beta_0$  and an allowed shape for  $\beta_1$ .

sition ( $e/\gamma > 30$ ), the  $\gamma$  rays of 142.6 keV do not contribute appreciably to the intensity measurement of the 140.5-keV  $\gamma$  rays. The source strength derived was  $(5.45 \pm 0.25) \times 10^8$ /sec or  $14.7 \pm 0.7$  mCi at the beginning of the  $\beta$ -ray spectrum measurements. This was about  $\frac{1}{3}$  of the total sample supplied. The error in this measurement is due mainly to uncertainty in the detector efficiencies. The uncertainty in the  $^{99}\text{Tc}^m$  half-life contributes an error of only 0.5% when correcting for a decay of 27 h.

#### C. Half-life for $\beta$ decay

As a check on the origin of the  $\beta$ -ray spectrum, measurements using a separate source of  $^{99}\text{Tc}^m$  were made on the rate of decay of the  $\beta$ -ray yield. For this test the spectrometer was focused first at an energy of 250 keV, and then beyond the end point for the background rate, and periodic counts were taken over a span of about 10 hours. An exponential decay of the net yield was observed with a half-life of  $5.9 \pm 0.2$  h. This confirms that

the  $\beta$  rays are indeed associated with 6.02-h  $^{99}\text{Tc}^m$  and not with a contaminant. Also, it should be noted that decay corrections to all points in the final runs were consistent with each other when the 6.02-h half-life was used.

#### D. $\gamma$ -ray measurements

The experimental arrangement for the  $\gamma$ -ray measurements consisted of placing a very strong source of  $^{99}\text{Tc}^m$  (initial strength about 250 mCi) on the axis of the Ge(Li) detector at a distance of 12 cm. Pb shielding enclosed the detector except for a line-of-sight opening to the source. The source was prepared by evaporating a saline sample to dryness ( $\sim 1.3$  cm diameter) on an aluminum backing, covering the material with one layer of Scotch tape and firmly securing the source to a Pb brick.

For the initial measurement, Pb absorbers totaling 0.543 cm in thickness were placed between the source and detector. All of the Pb attenuators used for these measurements were from a calibrated set of absorbers. While this initial amount of lead reduced the 140-keV  $\gamma$ -ray intensity by a calculated factor of  $4 \times 10^{-7}$ , the 233- and 322-keV  $\gamma$ -ray intensities were expected to be reduced by factors of 0.0128 and 0.1177, respectively. In these calculations  $\gamma$ -ray absorption coefficients in Pb were taken from the most recent tables<sup>11</sup> and a computer program was used that integrated over the solid angle subtended by the detector, including the absorption coefficient of  $\gamma$  rays in Ge. Figure 2 shows the relevant portions of the  $\gamma$ -ray spectrum obtained in the initial measurement. The low-energy region containing the relatively strong x-ray lines from Pb

has been omitted. A clear peak occurs at 233 keV along with another at 239 keV (nondecaying) ascribed to the decay of  $^{212}\text{Pb}$  from the surrounding Pb. The 233-keV peak, observed over a period of 12 h, decayed with the  $^{99}\text{Tc}^m$  half-life. Initial net counting rates for the 140-, 233-, and 322-keV peaks were 28.2,  $2.37 \times 10^{-2}$ , and 1.82 cts/sec for this geometry. By using the  $^{212}\text{Pb}$  peak energy of 238.63 keV (Ref. 1) as a calibrator, the energy of the  $^{99}\text{Tc}^m$  line is  $232.8 \pm 0.2$  keV, in good agreement with the value of  $232.70 \pm 0.15$  keV measured in the decay of  $^{99}\text{Rh}$ .<sup>1</sup>

After a delay of 68.8 h, during which time the source had decayed by a factor of  $3.64 \times 10^{-4}$ , the spectrum was again recorded, but with only 0.0721 cm of Pb absorber. This reduced the 140-keV  $\gamma$ -ray intensity by a calculated factor of 0.1425. Because the total counting rate was then 2800/sec, a 60-cycle pulser line was added to the spectrum so as to make a correction for analyzer deadtime that turned out to be 4.5%.

In order to calculate the relative  $\gamma$ -ray intensities the 233- and 322-keV net peak counting rates were used from the initial runs and the 140-keV net peak rate was used from the final run. Corrections were made for  $\gamma$ -ray attenuation in the Pb absorbers, relative  $\gamma$ -ray peak efficiencies based on the  $^{169}\text{Yb}$  measurements ( $\epsilon_{322}$  was about a factor of 2 lower than  $\epsilon_{140}$ ), decay, and, in the case of the final run, for analyzer dead-time. The error due to uncertainty in the relative absorption factors for the 322-keV  $\gamma$  rays in the first run and the 140-keV  $\gamma$  rays in the final run was estimated to be 6%. The  $^{99}\text{Tc}^m$  half-life value of  $6.02 \pm 0.01$  h leads to an uncertainty of only 1.3% in the relative source

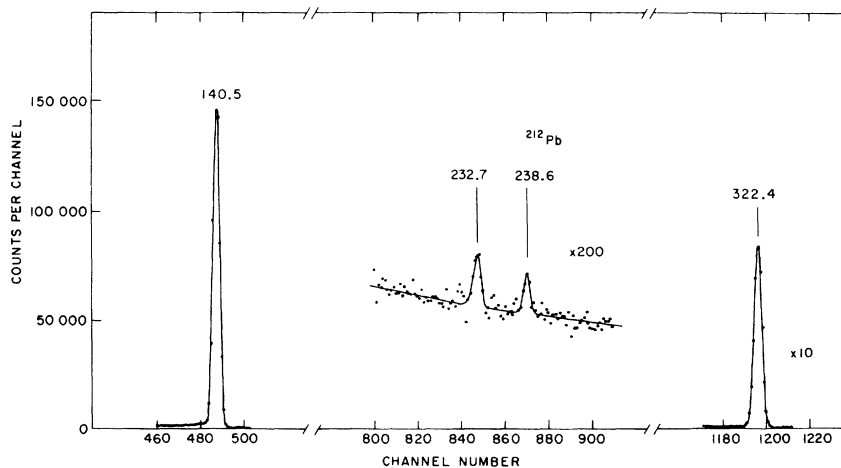


FIG. 2. Regions of the three  $\gamma$ -ray peaks from the decay of  $^{99}\text{Tc}^m$  as recorded in a Ge(Li) detector over a period of 11 h. A Pb attenuator 0.543 cm thick was located between the detector and a source of initial strength  $\sim 250$  mCi. The 238.6-keV peak is from  $^{212}\text{Pb}$  contamination in the Pb shielding. Energy values are from Ref. 1.

strength after 68.8 h. A further uncertainty of 4.1% in the relative  $\gamma$ -ray peak efficiencies of the Ge(Li) detector over the region 140 to 322 keV was estimated. By combining the various sources of error in quadrature the relative  $\gamma$ -ray intensities emitted by the source are as follows:  $I_{322}:I_{233}:I_{140} = (1.13 \pm 0.09) \times 10^{-6} : (0.95 \pm 0.17) \times 10^{-7} : 1.000$ .

#### IV. ANALYSIS OF THE $\beta$ -RAY SPECTRUM

A normal Kurie plot analysis of the  $\beta$  spectrum data points in Fig. 1(a) was made using tables<sup>12</sup> of Fermi functions for  $\beta^-$  emission to the  $Z = 44$  daughter. This plot had a clearly visible break showing that not only did the spectrum extend up to an energy of about 436 keV but that two components were present. According to the known energy level information<sup>1</sup> for the  $^{99}\text{Tc}^m$ - $^{99}\text{Ru}$  decay, the ground-state  $\beta$ -ray branch has a spin change of 2 and a parity change and must therefore be classified as a unique first-forbidden transition. Such transitions have a  $\beta$ -ray spectrum with a characteristic shape<sup>13</sup> which causes a curvature in the normal Kurie plot due to the fact that the maximum in such a spectrum occurs at a higher energy than in an allowed spectrum. The normal procedure is to correct the allowed Kurie plot data by the factor  $(1/\alpha)^{1/2}$  where  $\alpha = (W^2 - 1) + (W_0 - W)^2$ . Here  $W_0 = 1 + E_{\beta_{\text{max}}}(\text{keV})/511$  and  $W = 1 + E_{\beta}(\text{keV})/511$ . Application of this factor straightens out the forbidden Kurie plot and simplifies the analysis. Since all of the unique first-forbidden spectra ever measured<sup>13</sup> have had the  $\alpha$  shape, the use of this factor is fully justified. On the other hand, the  $\beta$ -ray branch of  $^{99}\text{Tc}^m$  to the  $^{99}\text{Ru}$  90-keV first-excited state has a spin change of 1 and a parity change, so it is classified as nonunique first forbidden. As discussed in Ref. 13, p. 1380, such spectra usually have the allowed shape due to the dominance of the energy-independent Coulomb term in the matrix element. Thus, the procedure adopted was to use the seven data points above 347 keV in Fig. 1(a) to form an  $\alpha$ -corrected Kurie plot. The end point thus obtained was  $434.8 \pm 2.6$  keV, where the overall error includes the error in the computer fitting together with the uncertainty in the spectrometer calibration. In Fig. 1(a) the curve labeled  $\beta_0$  is the complete spectrum constructed from the linear extrapolation of the  $\alpha$ -corrected Kurie plot of Fig. 1(b). This curve was then subtracted from the total spectrum data points and an allowed Kurie plot for the remainder was calculated as shown by the line  $\beta_1$  in Fig. 1(b). The computer fit to these data gave an end-point energy of  $346.7 \pm 2.0$  keV, again including the error in the spectrometer calibration.

In Fig. 1(a) the  $\beta_1$  spectrum was constructed from a linear extrapolation of the  $\beta_1$  Kurie plot.

From an analysis of the areas under the separate  $\beta_0$  and  $\beta_1$  spectra, carried out on the corresponding plots of counts per unit momentum interval versus momentum, the relative intensities were such that  $\beta_0$  is 28% of the total and  $\beta_1$  is 72%. The importance of assuming the  $\alpha$  shape for  $\beta_0$  was demonstrated by repeating the analysis using allowed shapes for both  $\beta_0$  and  $\beta_1$ . In this case the derived end-point energy of  $\beta_0$  was somewhat higher, as expected, i.e.,  $439.1 \pm 2.0$  keV, but still in fair agreement with the expected end point of 436.2 keV. In the energy region of the fit above 347 keV there was no noticeable difference in the quality of the fit as compared with the  $\alpha$  shape. However, the relative intensities derived were substantially different, i.e., 48% for  $\beta_0$  and 52% for  $\beta_1$ . This happens because the maximum of an allowed spectrum is at a lower energy and the spectrum, fitted only near the end point, rises to a higher level when extrapolated down in energy than in the case of the  $\alpha$  shape. In spite of the difference in the intensity ratios of  $\beta_0$  and  $\beta_1$  in the two analyses, the total intensities were nearly the same.

In the analysis of the  $\beta$  spectrum the effects of source thickness and back scattering from the source support foil could not be taken into account since there was essentially no experimental access to the low-energy region where such effects are usually observed. These effects increase the yield at low energies above what would be observed in the absence of scattering, but in most cases of past  $\beta$ -ray measurements the effect over the upper half of the spectrum has been small. Nevertheless, there is some residual uncertainty in this fitting analysis due to the limited region of the total spectrum that could be measured and the even more limited region for the fitting of the  $\beta_0$  component.

In order to derive the  $\beta$  branching intensities of  $^{99}\text{Tc}^m$ , the total spectrum, on a plot of counts per unit momentum interval versus momentum, was analyzed to determine the fraction of it that was detected within the instrumental linewidth when the spectrometer was focused at an energy of 210 keV. Based on the FWHM noted earlier this fraction was  $3.51 \pm 0.35\%$ . By combining this with the  $^{99}\text{Tc}^m$  net counting rate of 45.2/sec at 210-keV focusing energy, and the spectrometer transmission of 6.6% of  $4\pi$ , the total  $\beta$ -ray emission rate was found to be  $1.95 \times 10^4$ /sec. Together with the source strength of  $5.45 \times 10^8$ /sec the total  $\beta_0 + \beta_1$  branching intensity is then  $(3.6 \pm 0.6) \times 10^{-5}$  per decay where the various sources of error previously discussed have been combined in quadrature. Relative branching

based on the Kurie plot fitting analysis then leads to the adopted individual branches of  $(1.0 \pm 0.3) \times 10^{-5}$  for  $\beta_0$  and  $(2.6 \pm 0.5) \times 10^{-5}$  for  $\beta_1$ . Here the errors have been enlarged in order to allow for the uncertainties in the fitting including the possible effects of scattering.

### V. DISCUSSION

The ratio of the 322- and 140-keV  $\gamma$ -ray intensities from the present work agrees very well with the previous measurements by Jones and Griffin<sup>3</sup> and Décombaz *et al.*<sup>4</sup> The weighted mean of the three values is  $I_{322}/I_{140} = (1.10 \pm 0.06) \times 10^{-6}$ . From the relative intensity of the 233-keV  $\gamma$  rays, observed here for the first time in  $^{99}\text{Tc}^m$  decay, the  $\gamma$ -ray branches from the 322-keV state of  $^{99}\text{Ru}$  may be derived. The resulting branches are  $92 \pm 2\%$  for  $322 \rightarrow 0$  and  $8 \pm 2\%$  for  $322 \rightarrow 90$ , where small corrections have been made to the ratio of  $\gamma$ -ray intensities  $I_{233}/I_{322}$  for the respective previously measured<sup>1</sup>  $K$ -shell internal conversion plus an estimate of the total conversion in other shells. These  $\gamma$  branches agree very well with those of 93% and 7% obtained from the decay of  $^{99}\text{Rh}$  to the 322-keV state.<sup>1</sup>

In order to derive the  $\beta$ -ray branching to the 322-keV state, the  $\gamma$ -ray intensity ratio  $I_{322}/I_{140}$  of  $(1.10 \pm 0.06) \times 10^{-6}$  was corrected for (1) the fraction 0.894 of 140.5-keV  $\gamma$  rays per transition, (2) the 140.5-keV transition branching of 0.986 per decay, (3) the  $\gamma$  branching  $322 \rightarrow 0$  of 0.93, and (4) an additional correction of 1% for the total internal conversion of the 322-keV transition. The fully corrected value adopted for the  $\beta$ -ray branching of  $^{99}\text{Tc}^m$  to the 322-keV state is  $(1.05 \pm 0.06) \times 10^{-6}$  per decay.

The present results combined with previous information leads to the proposed decay scheme for  $^{99}\text{Tc}^m$  shown in Fig. 3. All possible  $\gamma$ - and  $\beta$ -ray decay modes of  $^{99}\text{Tc}^m$  apparently have now been observed either directly or indirectly. Table I further summarizes the results and also gives the  $\log ft$  values for the  $\beta$ -ray branches obtained by using calculated  $\log f^-$  values.<sup>14</sup> Here the  $f^-$ -value associated with unique first-forbidden decay, i.e.,  $f_1^-$ , has been used for the branches to the  $^{99}\text{Ru}$  ground and 322-keV states whereas  $f_0^-$  has been used for the  $\beta$  branch to the 90-keV state. The resulting  $\log ft$  values given in the last column of Table I for the branches to the ground and 90-keV states are within the ranges expected<sup>15</sup> for first-forbidden unique and nonunique  $\beta$ -ray transitions, respectively. Thus we may compare  $\log f_1^- t = 9.39$  for the ground-state  $\beta$  with the average<sup>15</sup>  $\log f_1^- t$  for the unique first-forbidden transitions of 9.7. However, the  $\log f_1^- t$  value of

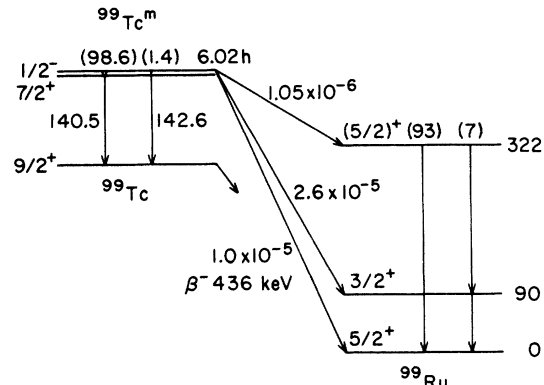


FIG. 3. Proposed decay scheme of  $^{99}\text{Tc}^m$ .  $\beta$ -ray branches to the  $^{99}\text{Ru}$  ground and 90-keV states are from the present results. For the  $\beta$ -ray branch to the 322-keV state the present result was combined with those of Refs. 3 and 4. All other information is from previous work. Numbers in parentheses are transition branching ratios in percent.

7.79 for the branch to the 322-keV state does not agree with the rule<sup>15</sup> that "first-forbidden unique  $\beta$  transitions have  $\log f_1^- t \geq 8.5$ ." In view of the present confirmation of the  $\beta$  branching intensity of  $10^{-6}$  to the 322-keV state, and thus the derived  $\log ft$  value, the explanation of the discrepancy might be that the spin of the state is  $\frac{1}{2}$  or  $\frac{3}{2}$  rather than  $\frac{5}{2}$ , making the  $\beta$  transition nonunique first forbidden. The only alternative, if the spin assignment of  $\frac{5}{2}$  is to be retained, is that this  $\log ft$  value is an exception to the rule. Further experimental evidence bearing on this point would be useful.

We may now consider the effect of the  $\beta$ -ray branches on dosage calculations in nuclear medicine applications. The mean energy of the  $\beta$  rays from the two main branches is about 150 keV. These branches have an intensity of  $3.6 \times 10^{-5}$  which is to be compared with the principal source of energetic electrons, namely the internal conversion of the electromagnetic transitions in  $^{99}\text{Tc}^m$  decay. As mentioned in the Introduction, the 140.5-keV transition undergoes internal conversion in 10.6% of its decays. Added to this is the 1.4%  $M4$  crossover transition of 142.6 keV (see Fig. 3) which is almost totally converted. This means that in nearly 12% of all  $^{99}\text{Tc}^m$  decays the emission consists of an energetic internal conversion electron. In Tc the  $K$ -shell binding energy is 21 keV and the  $L$  shells are bound by about 3 keV. Thus the internal conversion spectrum from  $^{99}\text{Tc}^m$  consists mainly of electrons of about 120 keV with some weaker lines extending up to nearly 140 keV. The mean energy is therefore slightly less than the ~150 keV mean energy of the  $\beta$ -ray spectrum discussed above.

TABLE I.  $\beta$ -ray branching of  $^{99}\text{Tc}^m$  ( $J^\pi = \frac{1}{2}^-$ ). Branches to the ground and 90-keV states of  $^{99}\text{Ru}$  are from the present work.

State of $^{99}\text{Ru}$ (keV)	$J^\pi$	Expected $E_{\beta_{\text{max}}}$ (keV)	Measured $E_{\beta_{\text{max}}}$ (keV)	$\beta$ branch (per decay)	$\log ft$
0	$\frac{5}{2}^+$	436.2	$434.8 \pm 2.6$	$(1.0 \pm 0.3) \times 10^{-6}$	$9.39 \pm 0.11^a$
90	$\frac{3}{2}^+$	346.4	$346.7 \pm 2.0$	$(2.6 \pm 0.5) \times 10^{-6}$	$8.66 \pm 0.08^b$
322	$(\frac{5}{2})^+$	113.8		$(1.05 \pm 0.06) \times 10^{-6}^c$	$7.79 \pm 0.03^a$

<sup>a</sup> $\log f_1 t$ .

<sup>b</sup> $\log f_0 t$ .

<sup>c</sup>Weighted average of the present result with those of Refs. 3 and 4.

But the intensity of the total  $\beta$ -ray spectrum is only  $3 \times 10^{-4}$  as great as the intensity of the internal conversion electrons. This is smaller than the accuracy with which the internal conversion intensity is known. We conclude that the additional dosage effect due to  $\beta$ -ray emission from  $^{99}\text{Tc}^m$  is negligible.

#### ACKNOWLEDGMENTS

We would like to thank E. K. Warburton for

helpful discussions. The computer program for calculating the  $\gamma$ -ray absorption factors was prepared by D. H. Wilkinson. We also thank E. der Mateosian for the loan of the set of calibrated Pb absorbers and A. W. Sunyar for preparation of the  $^{169}\text{Yb}$  calibration source. This research was supported by the Division of Basic Energy Sciences and the Office of Health and Environmental Research, U. S. Department of Energy, under Contract No. EY-76-C-02-0016.

<sup>1</sup>Table of Isotopes, 7th edition, edited by C. M. Lederer and V. S. Shirley (Wiley, New York, 1978).

<sup>2</sup>Radiopharmaceuticals, edited by G. Subramanian, B. A. Rhodes, J. F. Cooper, and V. J. Sodd (The Society of Nuclear Medicine, New York, 1975), and references cited therein.

<sup>3</sup>J. D. Jones and H. C. Griffin, Radiochem. Radioanal. Lett. **4**, 381 (1970).

<sup>4</sup>M. Décombaz, J. J. Gostely, and P. Lerch, Radiochem. Radioanal. Lett. **10**, 119 (1972).

<sup>5</sup>An intensity ratio  $I_{(322)}/I_{(140)}$  "in the order of  $6 \times 10^{-6}$ " was reported by I. L. Preiss, A. S. Frank, and R. Kishore, in Proceedings of the Second International Symposium on Radiopharmaceuticals, Seattle, Washington, 1979 (unpublished). Although this is stated to be in agreement with Ref. 4, there appears to be a factor of 6 difference. This value has not been included in deriving the mean.

<sup>6</sup>D. E. Alburger, P. Richards, and T. H. Ku, Int. J. Appl. Radiat. Isotopes (to be published).

<sup>7</sup>D. E. Alburger, Rev. Sci. Instrum. **27**, 991 (1956).

<sup>8</sup>F. P. Calaprice and D. E. Alburger, Phys. Rev. C **17**, 730 (1978).

<sup>9</sup>D. E. Alburger and E. K. Warburton, Phys. Rev. C **20**, 793 (1979).

<sup>10</sup>Calculations by J. W. Olness (private communication) based on absolute total efficiencies from S. H. Vegors, L. L. Marsden, and R. L. Heath, Phillips Petroleum Company Report No. IDO 16370, 1958 (unpublished), and peak-to-total ratios from F. C. Young, U. Maryland (unpublished).

<sup>11</sup>E. Storm and H. I. Israel, Nucl. Data Tables **A7**, 565 (1970).

<sup>12</sup>Tables for the Analysis of Beta Spectra, National Bureau of Standards Series 13, 1952 (unpublished).

<sup>13</sup>C. S. Wu, in *Alpha-, Beta-, and Gamma-Ray Spectroscopy*, edited by K. Siegbahn (North-Holland, Amsterdam, 1965), Vol. 2, pp. 1372-1376.

<sup>14</sup>N. B. Gove and M. J. Martin, Nucl. Data **A10**, 205 (1971).

<sup>15</sup>S. Raman and N. B. Gove, Phys. Rev. C **7**, 1995 (1973).